



PIERRE
AUGER
OBSERVATORY

A graphic for the ICRC 2019 logo, consisting of several blue lines radiating from a point at the top left, some solid and some dashed, creating a starburst or particle track effect.

ICRC2019

Madison, WI, USA

Mass Composition of Cosmic Rays with Energies above $10^{17.2}$ eV from the Hybrid Data of the Pierre Auger Observatory

Alexey Yushkov* for the Pierre Auger Observatory[†]

* Institute of Physics of the Czech Academy of Sciences

[†] Av. San Martín Norte 304, 5613 Malargüe, Argentina

http://www.auger.org/archive/authors_icrc_2019.html

Fluorescence Detector

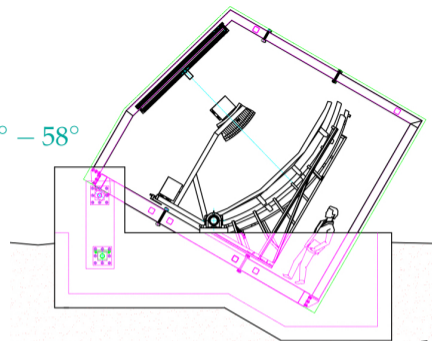
High elevation Auger telescopes

3 telescopes at Coihueco site

range of X_{\max} analysis: $10^{17.2} \text{ eV} < E < 10^{18.1} \text{ eV}$

data: same to ICRC (2017) [J. Bellido, PoS(ICRC2017)506]

elevation $30^\circ - 58^\circ$



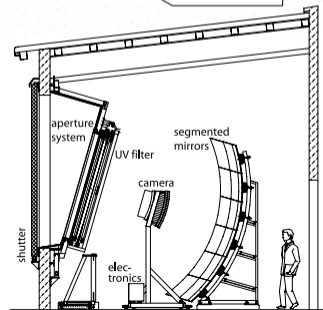
Standard telescopes

24 telescopes at 4 sites

range of X_{\max} analysis: $E > 10^{17.8} \text{ eV}$

compared to ICRC (2017): update with 2016 – 2017 (+20% of statistics)

elevation $1.5^\circ - 30^\circ$



Measurements of the depth of shower maximum X_{\max}

47863 high-quality events

1020 events with $E > 10$ EeV

the highest energy 104 ± 9.5 EeV

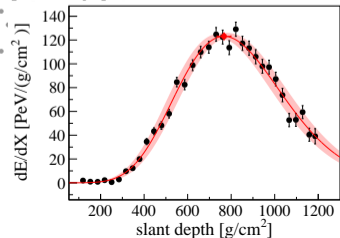
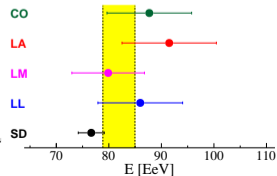
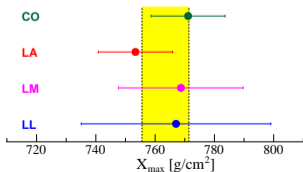
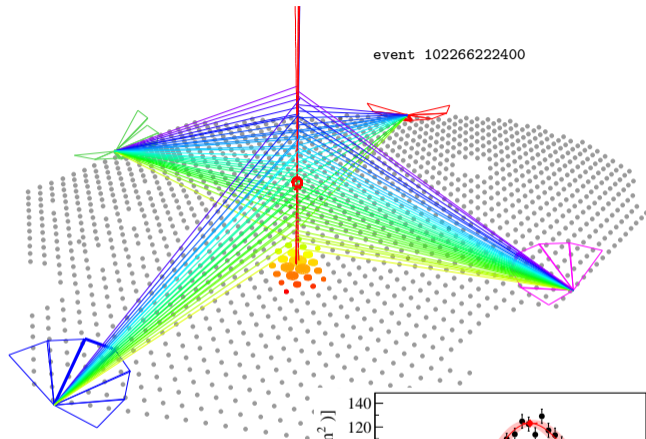
systematics $\lesssim 10 \text{ g cm}^{-2}$

resolution

40 g cm^{-2} at $10^{17.2} \text{ eV}$

25 g cm^{-2} at $10^{17.8} \text{ eV}$

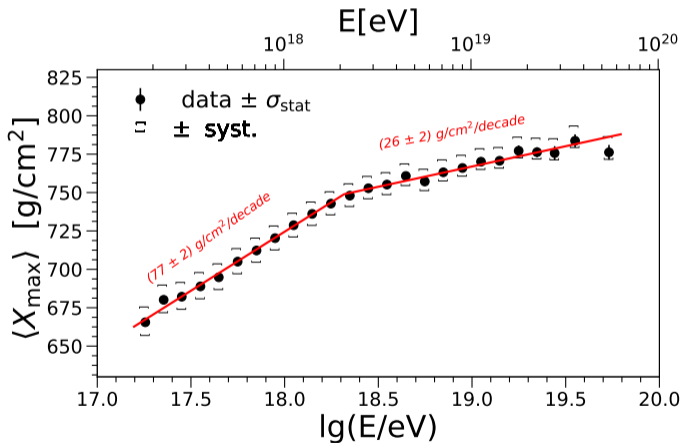
15 g cm^{-2} for $E > 10^{19.0} \text{ eV}$



Rate of change of X_{\max} with energy

One of the most reliable observables for mass composition analysis

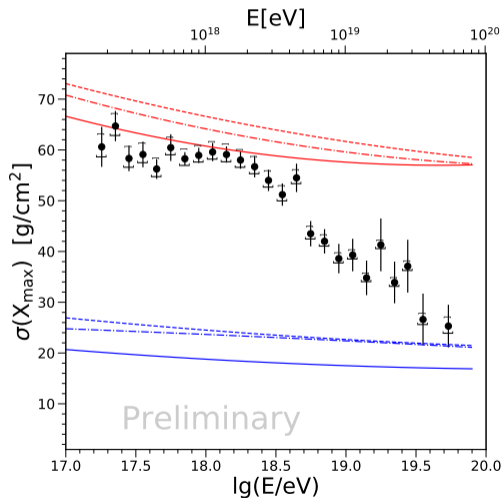
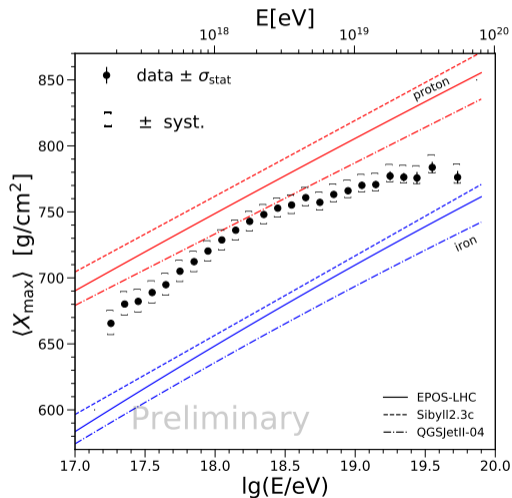
simulations: ≈ 60 [g cm⁻²/decade] for constant compositions



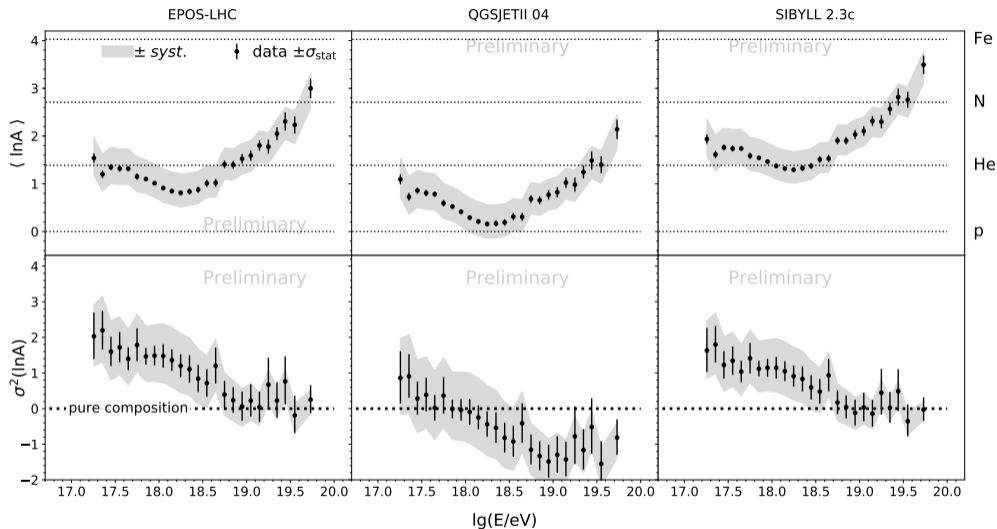
Composition is getting lighter below $E_0 \approx 2 \text{ EeV}$ and heavier afterwards

X_{\max} moments: data vs simulations

Above $E_0 \approx 2$ EeV both X_{\max} moments are becoming compatible to MC predictions for heavier nuclei



$\langle \ln A \rangle$ and $\sigma^2(\ln A)$ from first two moments of X_{\max} distributions



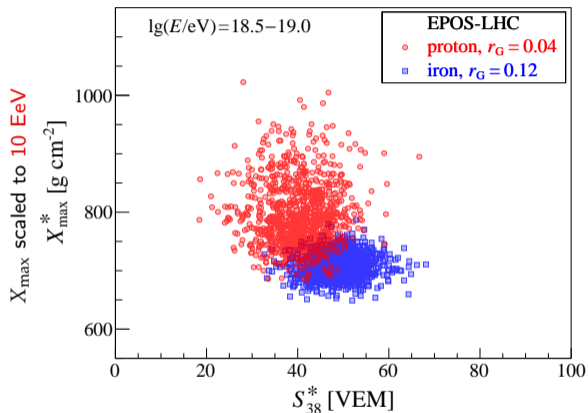
Model-independent decrease of $\sigma(\ln A)$ until $\sim 10^{18.7} \text{ eV}$

Less model-dependent constraints on $\sigma(\ln A)$ near the ankle?

Correlation between X_{\max} and signal in the surface detector

heavier nuclei produce shallower showers with larger signal (more muons)

general characteristics of air showers / minor model dependence

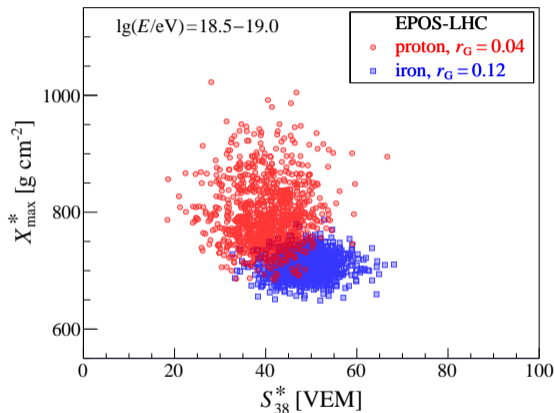


signal at 1000 m from the core scaled to 10 EeV, 38°

Correlation between X_{\max} and signal in the surface detector

heavier nuclei produce shallower showers with larger signal (more muons)

general characteristics of air showers / minor model dependence



Correlation for EPOS-LHC

pure beams $\sigma(\ln A) = 0$

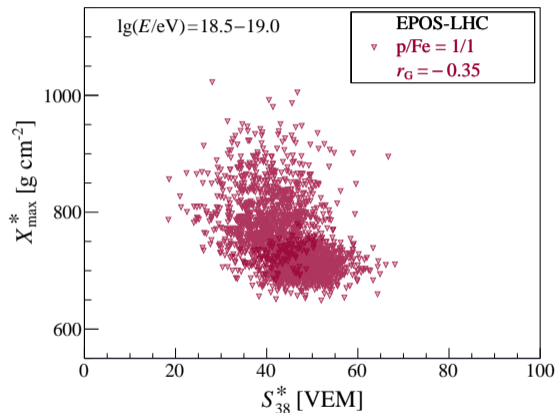
+0.04 for proton

+0.12 for iron

Correlation between X_{\max} and signal in the surface detector

heavier nuclei produce shallower showers with larger signal (more muons)

general characteristics of air showers / minor model dependence



Correlation for EPOS-LHC

pure beams $\sigma(\ln A) = 0$

+0.04 for proton

+0.12 for iron

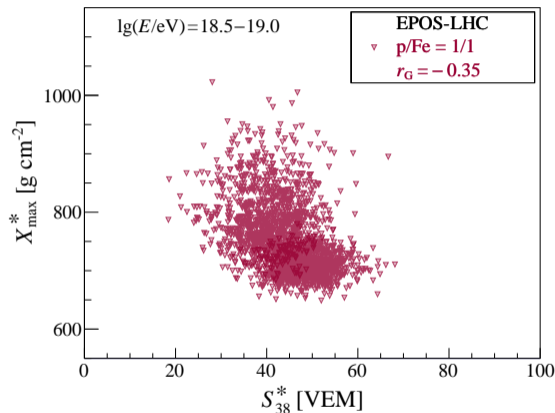
maximal mixing $\sigma(\ln A) \approx 2$

-0.35 for p/Fe= 1/1

Correlation between X_{\max} and signal in the surface detector

heavier nuclei produce shallower showers with larger signal (more muons)

general characteristics of air showers / minor model dependence



Correlation for EPOS-LHC

pure beams $\sigma(\ln A) = 0$

+0.04 for proton

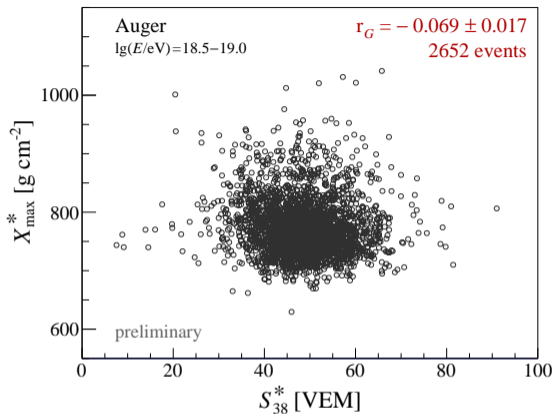
+0.12 for iron

maximal mixing $\sigma(\ln A) \approx 2$

-0.35 for p/Fe = 1/1

More negative correlation \Rightarrow more mixed composition

Correlation in data compared to pure beams



correlation for protons

EPOS-LHC

+0.04

QGSJetII-04

+0.12

Sibyll 2.3c

+0.04

difference to data

$\approx 6.0\sigma$

$\approx 11.0\sigma$

$\approx 6.0\sigma$

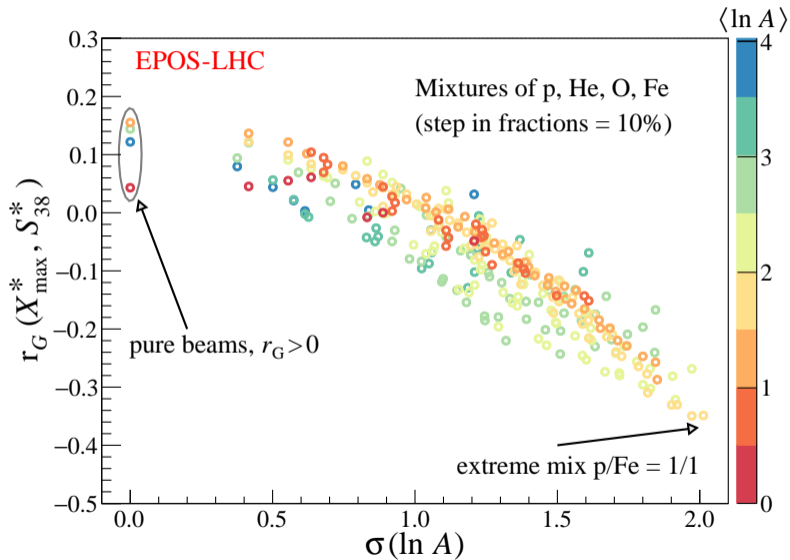
difference is larger for other pure beams

difference is $> 5\sigma$ for all p – He mixes

primary composition near the ankle is mixed
nuclei with $A > 4$ needed to explain data

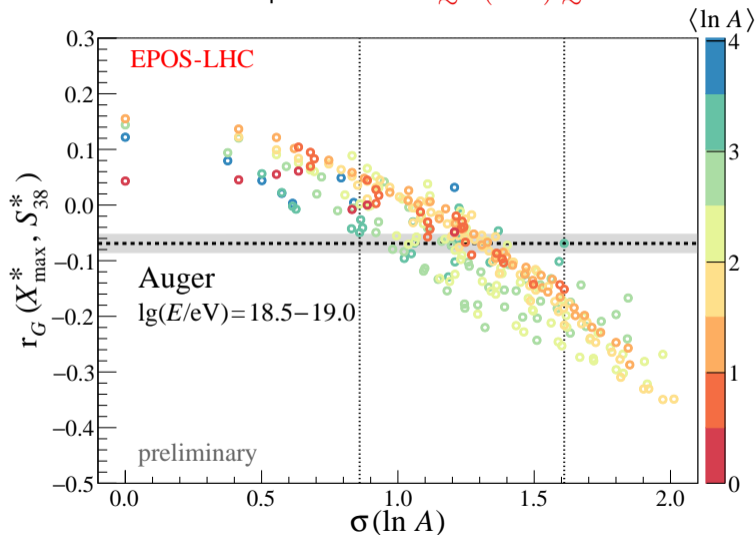
systematics plays only a minor role $\sigma_{\text{syst}}(r_G) \lesssim \begin{smallmatrix} +0.01 \\ -0.02 \end{smallmatrix}$

Dependence of correlation on $\sigma(\ln A)$



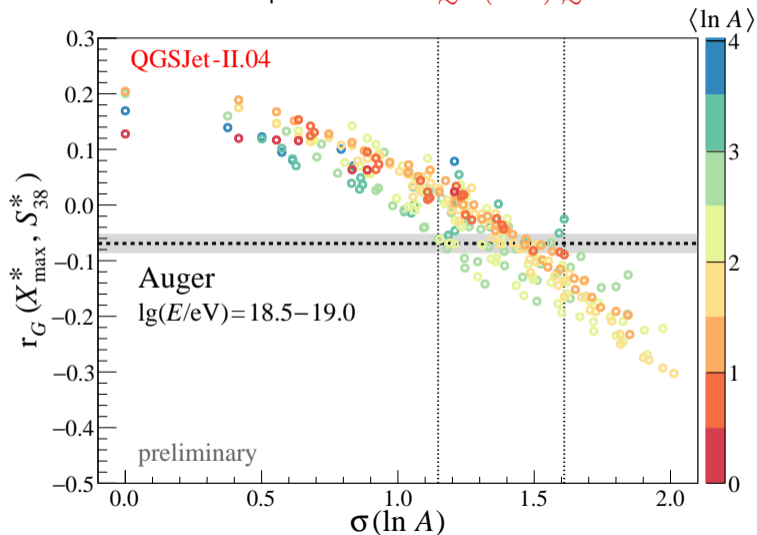
Constraints on $\sigma(\ln A)$ from observed $r_G(X_{\max}^*, S_{38}^*)$

Data are compatible to $0.85 \lesssim \sigma(\ln A) \lesssim 1.60$



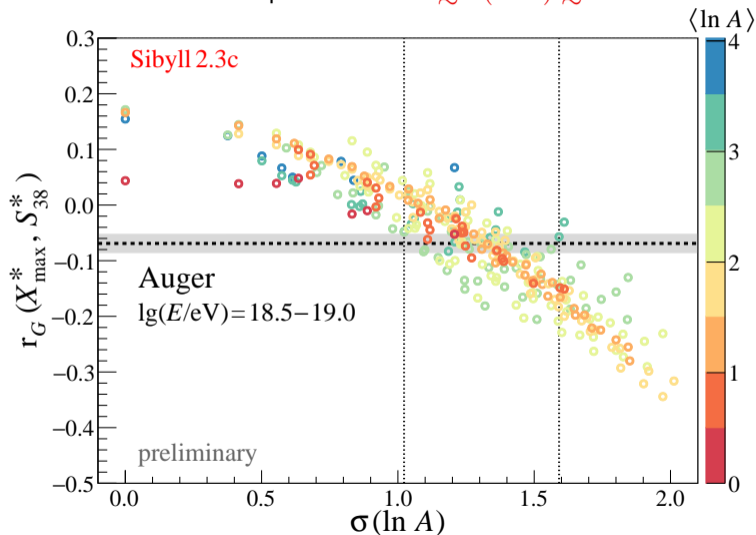
Constraints on $\sigma(\ln A)$ from observed $r_G(X_{\max}^*, S_{38}^*)$

Data are compatible to $0.85 \lesssim \sigma(\ln A) \lesssim 1.60$



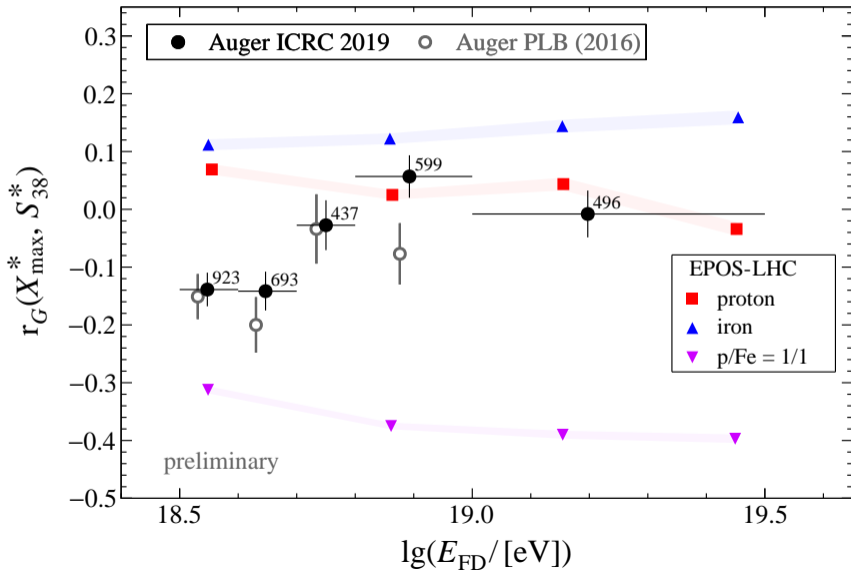
Constraints on $\sigma(\ln A)$ from observed $r_G(X_{\max}^*, S_{38}^*)$

Data are compatible to $0.85 \lesssim \sigma(\ln A) \lesssim 1.60$



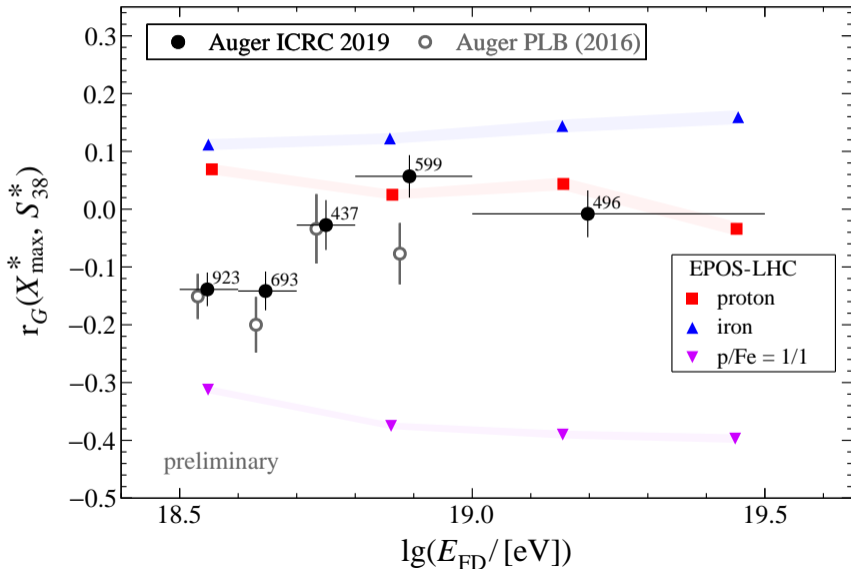
Energy dependence

new data are compatible to [Auger PLB 762 (2016)]: $\chi^2/\text{ndf} = 5.4/4$ (p-value = 0.25)



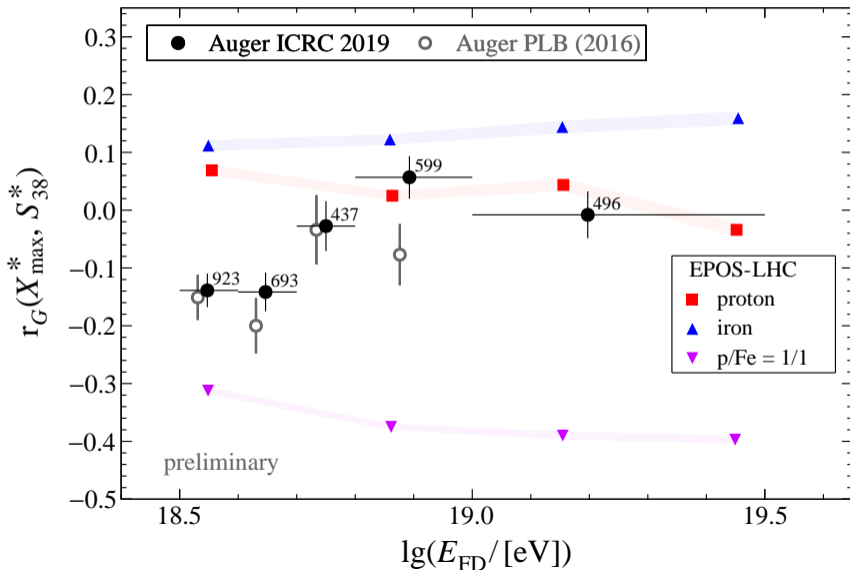
Energy dependence

$\lg(E/\text{eV}) = 18.5 - 18.7$ (1616 events): $r_G = -0.141 \pm 0.022$, at 6.4σ from zero

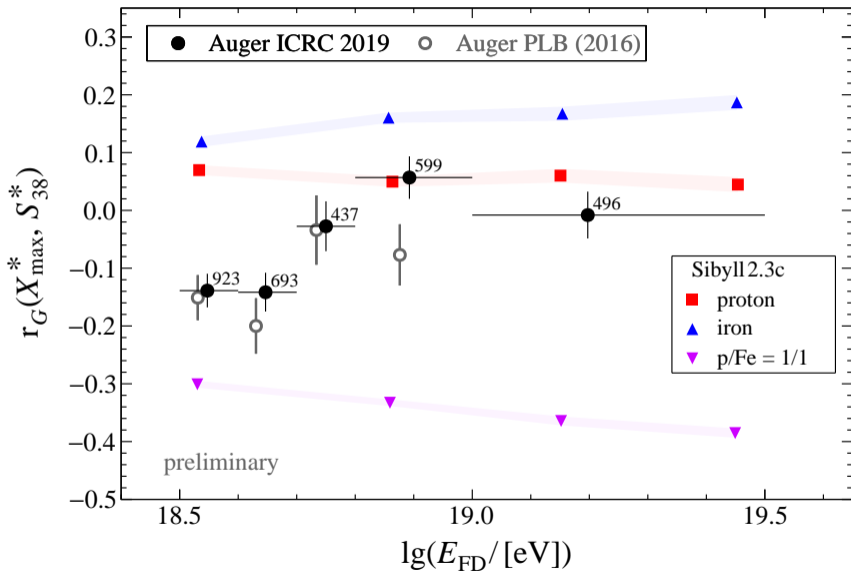


Energy dependence

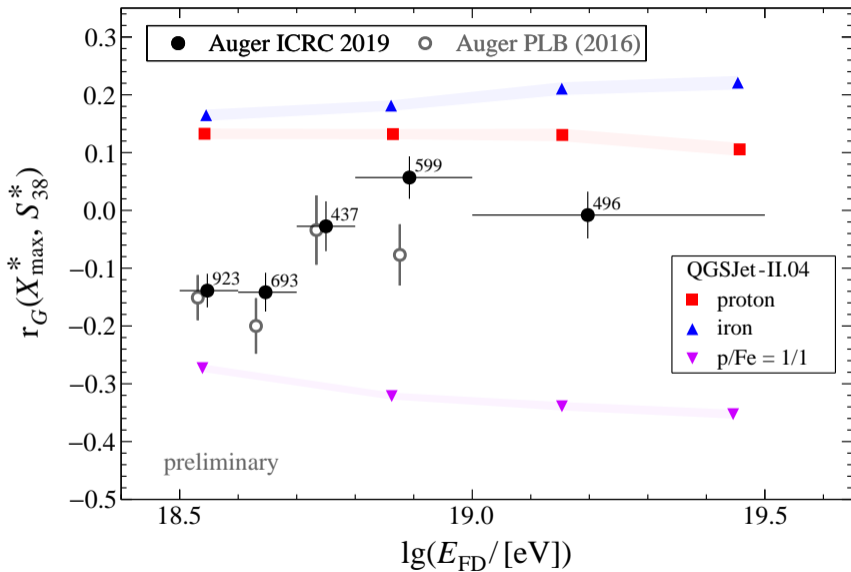
above the ankle $\lg(E/\text{eV}) > 18.7$ data are compatible to decrease of $\sigma(\ln A)$



Energy dependence



Energy dependence



Results (independent of the hadronic models)

X_{\max} analysis

$\langle \ln A \rangle$: decreasing up to 2 EeV and increasing afterwards

$\sigma(\ln A)$: decreasing up to the ankle, more constant at higher energies

$r_G(X_{\max}^*, S_{38}^*)$ analysis for $\lg(E/\text{eV}) = 18.5 - 19.0$

below the ankle the correlation in data is significantly, at 6.4σ from zero, negative

pure compositions and proton-helium mixes (all having $r_G > 0$) are excluded

data are compatible to mixed compositions with $\sigma(\ln A) = 0.85 - 1.60$

above the ankle there are indications on decrease of $\sigma(\ln A)$ (more statistics is needed)

backups

The Pierre Auger Observatory

Fluorescence detector (FD) [longitudinal profile]

duty cycle 15 %

24 + 3 fluorescence telescopes
at 4 locations

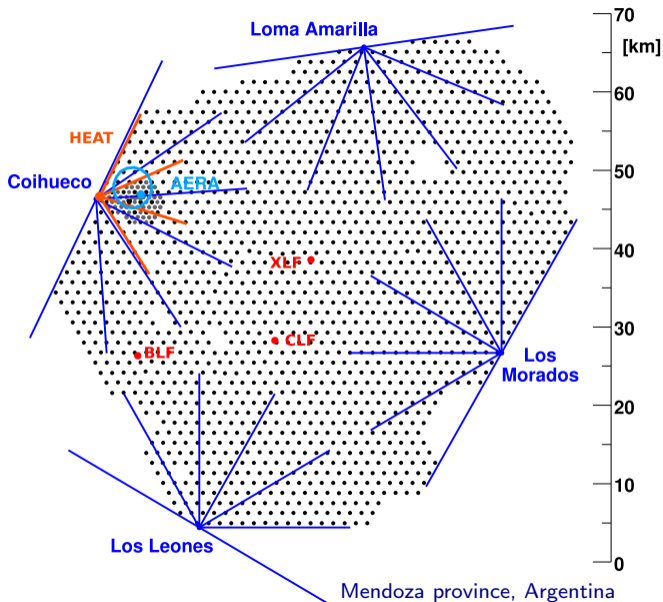
Surface detector (SD) [lateral distribution]

duty cycle 100 %

1660 water-Cherenkov stations
at 1500 m spacing, 3000 km²

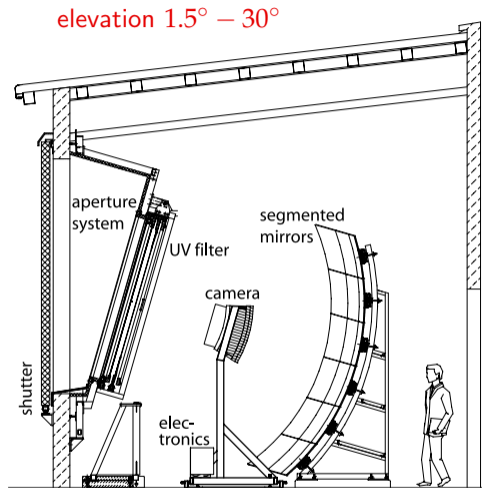
61 water-Cherenkov stations
at 750 m spacing, 23.5 km²

Nucl. Instrum. Meth. A798 (2015) 172



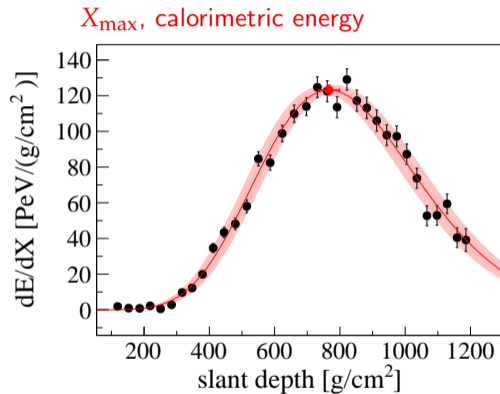
Fluorescence Detector

FD telescopes at Los Morados



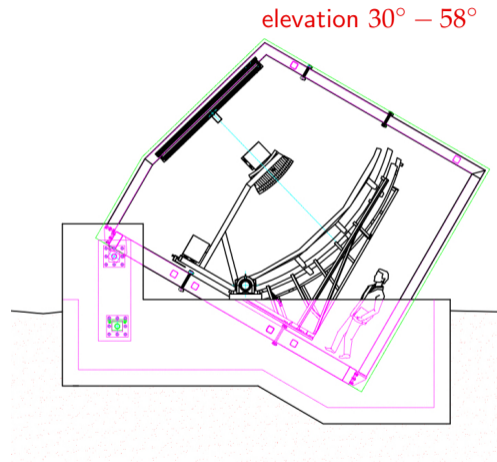
Fluorescence Detector

FD telescopes at Los Morados



High Elevation Auger Telescopes (HEAT)

Detection of showers with $E < 10^{18}$ eV

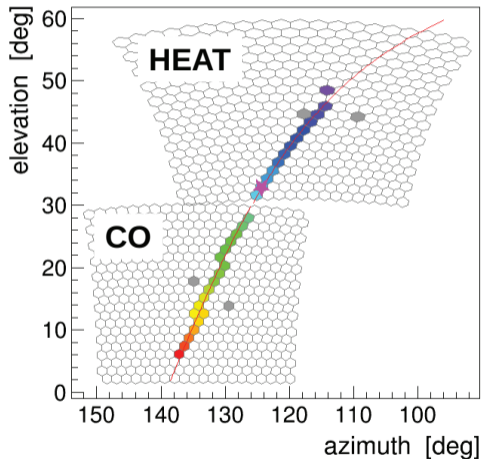


High Elevation Auger Telescopes (HEAT)

Detection of showers with $E < 10^{18}$ eV

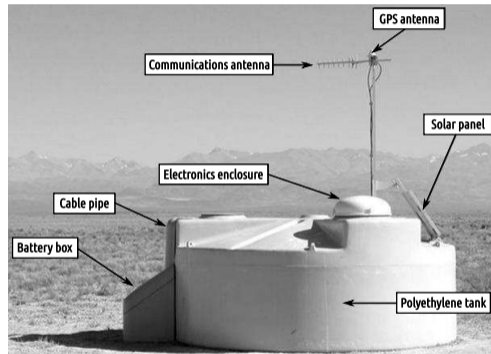


FOV combined with Coihueco FD site



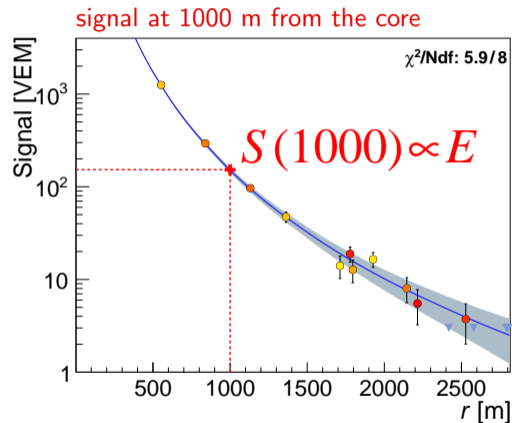
Surface detector

Water-Cherenkov station



Surface detector

Water-Cherenkov station



mass composition sensitivity: muons contribute from 40 to 90% to $S(1000)$ depending on zenith angle